PHYSICAL REVIEW B VOLUME 55, NUMBER 18 1 MAY 1997-II

Correlation effects in carbon nanotubes

Leon Balents and Matthew P. A. Fisher
Institute for Theoretical Physics, University of California, Santa Barbara, California 93106-4030
(Received 18 November 1996)

We consider the effects of Coulomb interactions on single-wall carbon nanotubes using an on-site Hubbard interaction, u. For the (N,N) armchair tubes the low-energy theory is shown to be *identical* to a two-chain Hubbard model at *half-filling*, with an effective interaction $u_N = u/N$. Umklapp scattering leads to gaps in the spectrum of charge and spin excitations which are exponentially small for large N. Above the gaps the intrinsic nanotube resistivity due to these scattering processes is linear in temperature, as observed experimentally. The presence of ''d-wave'' superconductivity in the two-chain Hubbard model away from half-filling suggests that *doped* armchair nanotubes might exhibit superconductivity with a purely electronic mechanism. [S0163-1829(97)50518-2]

Carbon nanotubes constitute a novel class of quasi-one-dimensional (1D) materials which offer the potential for both new physics and technology.[1] Although built only with carbon atoms, they can be grown in a tremendous variety of shapes and sizes. The simplest single-wall tube consists of a single graphite sheet which is curved into a long cylinder, with a diameter which can be smaller than 1 nm. Several groups[2] have succeeded in measuring the resistance of a *single* multiwall nanotube, composed of several concentric cylinders. Crystalline ''ropes'' consisting of a triangular packing of (nominally) identical single-wall tubes are also very promising, exhibiting signatures of metallic transport.[3]

Generally, single-wall tubes can be characterized by two integers (N,M) which specify the superlattice translation vector which wraps around the waist of the cylinder. Current theories[4,5] consist of band-structure calculations and predict a rich variety of behavior, ranging from metallic ''armchair'' tubes with (N,N) to insulating ''zig-zag'' tubes with $(N,0)$. For very small nanotubes, however, electron correlation effects should become important, as in other 1D systems.[6] In this paper we study these effects using a tight-binding description (which correctly reproduces the band-structure calculations) supplemented by an on-site Hubbard interaction u. For the (N,N) armchair tubes we show that the effective description at low energies is *identical* to a two-chain Hubbard model at *half-filling* with an effective interaction strength, $u_N = u/N$. Since this effective interaction is weak for $N \sim 10$, its effects can be treated perturbatively. Particularly important are electronic Umklapp scattering processes, present at half-filling. These are predicted to open a small charge and spin gap, changing the behavior from metallic to insulating at low enough temperatures. Similar conclusions have been reached independently in very recent work by Krotov, Lee, and Louie.[7] At temperatures above the charge gap, a simple weak-coupling analysis of these interactions gives a resistivity which varies linearly with temperature, which may explain the observed behavior[3] in single carbon ''ropes.'' Furthermore, doping an armchair nanotube is equivalent to moving away from half-filling in the two-chain Hubbard model. This problem has been extensively studied,[8] and exhibits superconducting behavior at low temperatures, with a ''d-wave'' symmetry. This suggests a possible electronic mechanism for superconductivity in doped nanotubes.

Following various authors,[4] we first consider a single sheet of graphite, composed of carbon atoms arranged on the sites of a honeycomb lattice. The underlying Bravais lattice is triangular, with two sites per unit cell. The two primitive Bravais lattice vectors are $\vec{a}_\pm = (a/2)(\pm 1, \sqrt{3})$, where $a = \sqrt{3}d$, with d the near-neighbor carbon separation. Of the four outer-shell electrons of each atom, three form the sp_2 bonds of the lattice, while the fourth can tunnel between neighboring p_z orbitals. A simple description, which correctly accounts for the semimetallic behavior of graphite, consists of a tight-binding model with one p_z orbital per carbon, and a tunneling matrix element t between neighboring atoms. The Bloch states for this tight-binding model form two bands, with energies $E_\pm(\vec{k}) = \pm|\xi(\vec{k})|$ where

$$\xi(\vec{k}) = 2t\cos(k_x a/2)e^{ik_y a/2\sqrt{3}} + t_\perp e^{-ik_y a/\sqrt{3}}, \qquad (1)$$

and $\vec{k}$ is the crystal momentum. Here we have allowed for a different hopping strength, $t_\perp$, in the y direction (see Fig. 1). With one electron per carbon atom, the Fermi energy is at $E=0$, with the lower band full and the upper empty. The striking feature of this band structure is that there are two isolated points in the first Brillouin zone, denoted $\vec{K}_\pm$, where the bands touch $E=0$, and there are gapless excitations. In the vicinity of these ''Dirac'' points, for $\vec{q} = \vec{k} - \vec{K}_\pm$ small, the dispersion is relativistic, with $E(\vec{q}) = v|\vec{q}|$ and $v = (\sqrt{3}a/2)t$ (for $t_\perp = t$). When $t = t_\perp$, the gapless points occur at $\vec{K}_\pm = (\pm 4\pi/3a, 0)$, but are shifted along the k_x axis for $t \neq t_\perp$ (see Fig. 2).

Single-wall nantotubes consist of rolling the honeycomb sheet of carbon atoms into a cylinder. Each tube is characterized by two integers[4] (N,M), which specify the superlattice translation vector $T_{(N,M)} = N\vec{a}_+ + M\vec{a}_-$, which wraps around the waist of the cylinder. The crystal momentum transverse to the axis of the cylinder is then quantized. Band structure predicts[4] metallic behavior whenever the gapless points in the Brillouin zone lie on the allowed transverse

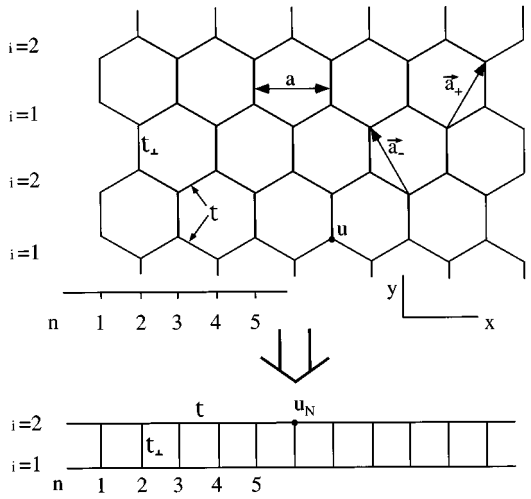

FIG. 1. Illustration of the graphite lattice, with labeling and periodic boundary conditions for an armchair tube.

quantized wave vectors. For the armchair nanotubes with (N,N) this is illustrated in Fig. 2(a), where the allowed values of k_y are shown as dashed lines for $N=4$. Since gapless modes are present at $k_y=0$, band structure predicts metallic behavior for armchair tubes, independent of N. Due to curvature effects,[5] the hopping matrix elements along (t) and around $(t_\perp)$ the nanotube will differ slightly, by an amount of order $1/N^2$. This shifts the Dirac points at $\vec{K}_\pm$ along k_x, but leaves the armchair tube gapless (metallic). For the $(N,-N)$ zig-zag tube [equivalent to the $(N,0)$ tube] with noninteger $N/3$, the gapless points do not coincide with quantized transverse momenta, so that insulating behavior is predicted with a gap varying as $1/N$. For integer $N/3$ the Dirac points for $t=t_\perp$ are at quantized transverse momenta, but are shifted away slightly, of order $1/N^2$, due to curvature effects[5] $(t\neq t_\perp)$. Thus band structure predicts semimetallic behavior for integer $N/3$ zig-zag tubes [Fig. 2(b)].

For the armchair tubes the low-energy modes occur near the two gapless points, at $k_y=0$. The 1D dispersion away from these two points is shown in Fig. 3. In addition there are gapped modes at $k_y\neq 0$, with an energy of order

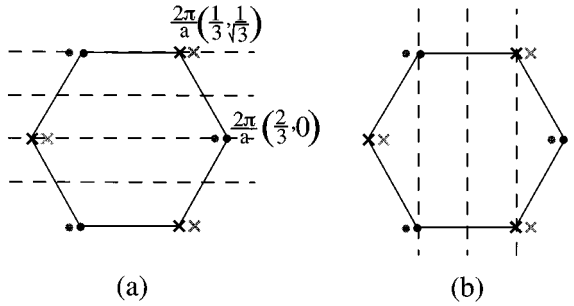

FIG. 2. Dirac points in the Brillouin zone. Dark circles and crosses indicate the locations of the gapless points for $t_\perp=t$, while gray symbols schematically indicate the shifted positions for $t_\perp<t$. Dashed lines cut the zone at a discrete set of allowed transverse momenta in (a) the armchair tube and (b) the zig-zag tube (here with $N=3$).

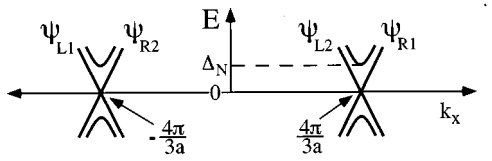

FIG. 3. One-dimensional spectrum near Dirac points.

$\Delta_N=2\pi v/(\sqrt{3}Na)=\pi t/N$ (for $t_\perp=t$). Below Δ_N, the mode structure is equivalent to a 1D two-band model, independent of the nanotube size N.

Coulomb interactions can be incorporated into the nanotube tight-binding model, and will introduce interactions into the effective 1D model. To be concrete we focus on an on-site Hubbard interaction u, so that the full Hamiltonian becomes

$$H=-\sum_{\langle \mathbf{r}\mathbf{r}'\rangle} t_{\mathbf{r}\mathbf{r}'} c_\alpha^\dagger(\mathbf{r}) c_\alpha(\mathbf{r}') + u\sum_{\mathbf{r}} n_\uparrow(\mathbf{r}) n_\downarrow(\mathbf{r}), \qquad (2)$$

where the first sum is over spin states $(\alpha=\uparrow,\downarrow)$ and near-neighbor sites of the honeycomb lattice, and $n_\alpha(\mathbf{r})=c_\alpha^\dagger(\mathbf{r})c_\alpha(\mathbf{r})$. We now show that for (N,N) armchair tubes the effective interacting 1D model is *identical* to a two-chain Hubbard model with an interaction strength, $u_N=u/N$. To do so, we choose a particular basis of states spanning the space of low-energy states with $k_y=0$:

$$\phi_{n1}(x,y)=\begin{cases} N^{-1/2}\delta_{x,na_0}\delta_{y,6\ell a_0/\sqrt{3}} & n \text{ even},\\ N^{-1/2}\delta_{x,na_0}\delta_{y,(6\ell+1)a_0/\sqrt{3}} & n \text{ odd}, \end{cases} \qquad (3)$$

$$\phi_{n2}(x,y)=\begin{cases} N^{-1/2}\delta_{x,na_0}\delta_{y,(6\ell-2)a_0/\sqrt{3}} & n \text{ even},\\ N^{-1/2}\delta_{x,na_0}\delta_{y,(6\ell+3)a_0/\sqrt{3}} & n \text{ odd}, \end{cases} \qquad (4)$$

where the second Kronecker delta function must be satisfied for some integer ℓ, and $a_0=a/2$. As indicated in Fig. 1, ϕ_{n1} and ϕ_{n2} are simply the two normalized basis states with uniform support at $x=na_0$ on even or odd chains, respectively. In the low-energy theory, we may restrict the expansion of the field operators to this basis:

$$c_\alpha^\dagger(\mathbf{r})=\sum_{ni}\phi_{ni}(\mathbf{r})c_{ni\alpha}^\dagger. \qquad (5)$$

Inserting this into the Hubbard Hamiltonian and summing over y for fixed x gives

$$H=\sum_n \{-t(c_{ni\alpha}^\dagger c_{n+1,i\alpha}+\text{H.c.})-t_\perp(c_{n1\alpha}^\dagger c_{n2\alpha}+\text{H.c.})\}$$

$$+u_N\sum_{ni} c_{ni\uparrow}^\dagger c_{ni\uparrow}c_{ni\downarrow}^\dagger c_{ni\downarrow}, \qquad (6)$$

which is precisely the Hamiltonian of the two-chain Hubbard model, but with an *effective* weak interaction $u_N=u/N$. The factor of $1/N$ arises because the electrons are delocalized around the circumference of the nanotube, and hence occupy the same site with a probability reduced by $1/N$.

A considerable amount is known about the two-chain Hubbard model,[8] particularly in the weak-coupling limit, where controlled renormalization group calculations may be

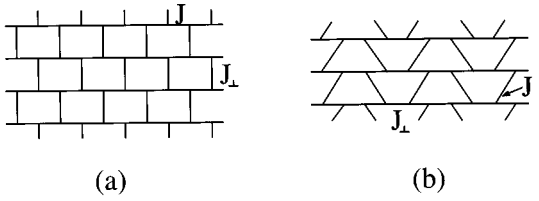

FIG. 4. Effective spin models for (a) the armchair tube and (b) the zig-zag tube.

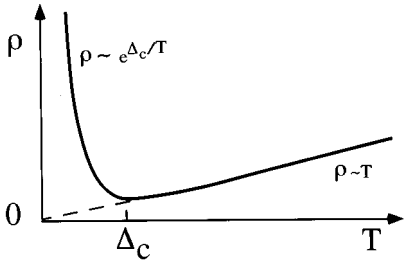

FIG. 5. Resistivity of an ideal armchair tube (schematic).

used. These methods proceed by diagonalizing the kinetic energy, linearizing the 1D spectrum near the resulting Fermi points, and expanding the Hubbard interactions in the basis of states of the resulting two bands. In the undoped case at half-filling, interactions drive an instability to a Mott-insulating spin liquid with a gap in both the charge *and* spin sectors. In the weak-coupling limit, $u_N \ll t$, both gaps are exponentially small: $\Delta \sim t\exp(-ct/u_N)$. At temperatures below the charge gap Δ_c, activated behavior is expected in the resistivity, $\rho \sim \exp(\Delta_c/k_B T)$, as illustrated schematically in Fig. 5. With increasing u_N the charge gap evolves continuously into the strong-coupling Mott gap associated with the energy cost of doubly occupying a site. The spin gap at strong coupling is more subtle, but indicates a quantum disordered or short-range resonating valence bond (RVB) ground state.[9] A spin gap is also present in a two-leg Heisenberg ladder, in contrast to a single chain which has gapless spin excitations.[10] For the armchair tubes the spin gap at strong coupling can be understood in terms of a Heisenberg spin model on the honeycomb network, which is topologically equivalent to the ''brick wall'' lattice shown in Fig. 4(a). In the anisotropic limit $J_\perp \gg J$, local spin singlets form along the vertical rungs, and there is a spin gap to triplet excitations.

Upon doping for $t_\perp \lesssim 2t$, the two-chain Hubbard model is known to undergo a phase transition into a state which retains the spin gap but develops power-law singlet superconducting (SS) and charge-density-wave (CDW) correlations.[8] Furthermore, the pair wave function associated with the SS correlator has approximate $d_{x^2-y^2}$ symmetry (i.e., a sign change from quadrant to quadrant in the k_x, k_y plane). Both theoretical and numerical studies[8,11] suggest that the SS correlations are enhanced over the CDW ones if the Fermi level is pushed into the proximity of a band edge. In weak coupling, the enhancement is mediated by scattering into the nearly empty/full band, for which the 1D van Hove singularity provides an enormous density of states. This suggests that for armchair tubes, superconducting effects might be maximized by tuning the doping so that the Fermi energy coincides with the lowest-lying ($k_y = \pm 2\pi/Na\sqrt{3}$) bands near the two Dirac points (see Fig. 3).

For $(N,-N)$ zig-zag tubes with integer $N/3$ the gapless Dirac points coincide with the discrete quantized momenta for $t = t_\perp$, see Fig. 2(b). However, due to curvature effects $t \neq t_\perp$, so that the gapless points are slightly shifted, leading to a small gap[5] of order $|t - t_\perp| \sim 1/N^2$. Since this is smaller than the effective interaction strength, which varies as $1/N$, it is probably legitimate to ignore this small shift when interactions are included. Even with this simplification, it is not possible to map the zig-zag tube directly into a two-chain Hubbard model. Nevertheless, proceeding by focusing on the two gapless modes and expressing the Hubbard interaction in terms of these, one obtains an effective interacting 1D two-band model for the zig-zag tube. Just as for the two-chain Hubbard model, this model has Umklapp scattering processes, but their particular strengths are different. It is natural to expect that these Umklapp processes will gap out both the charge and spin excitations, just as for the Hubbard model, although a definitive statement requires a detailed calculation. Since the $N=3$ zig-zag tube essentially consists of three real-space chains, a spin gap may seem surprising. Indeed, it is known[10] that conventional Heisenberg spin ladders with an *odd* number of legs have *gapless* spin excitations, in contrast to the spin-gapped even leg ladders. An important distinction, however, is the unusual topology of the strong coupling Heisenberg model for the zig-zag tube, as depicted in Fig. 4(b). In the anisotropic limit, $J_\perp \ll J$, spins on such a ''herringbone'' lattice will indeed form local singlets across the vertical bonds, with a spin gap.

Returning to the armchair tubes, since the effective interaction strength $u_N = u/N$, one expects correlation effects to be weak for large N. Indeed, as noted above, the gaps in the undoped case become exponentially small for $u_N \ll t$, and the scale for superconductivity will likewise be small, indicating the desirability of reducing the nanotube size in experiments.

Even for larger N (the weak-coupling limit), however, an interesting observable consequence of interaction physics should remain in the high-temperature resistivity. Indeed, Umklapp scattering leads to an intrinsic contribution to the scattering rate which in weak coupling varies *linearly* in T for $T \gtrsim \Delta_c$ in 1D (Ref. 12). This is a dramatic enhancement over the conventional Fermi-liquid T^2 resistivity, and can also be much larger than scattering due to (3D) phonons, which vanishes at least as fast as T^3. We now proceed to obtain a quantitative estimate of this effect.

The effective low-energy Hamiltonian for the (N,N) nanotube (and for the two-chain Hubbard model) consists of right and left moving electrons in the two bands:

$$H_0 = \sum_{a=1,2} \int dx [\psi^\dagger_{Ra} iv\partial_x \psi_{Ra} - \psi^\dagger_{La} iv\partial_x \psi_{La}], \qquad (7)$$

where we have suppressed the spin label. Since the equivalent two-chain Hubbard model is at half-filling, the presence of the Hubbard interaction, u_N, introduces Umklapp scattering, as well as numerous momentum conserving four-fermion interactions. The three Umklapp interactions, which scatter two right moving electrons into two left movers, take the form

$$H_U = u_N a_0 \int dx[\psi^\dagger_{L\uparrow}\psi^\dagger_{L\downarrow}\psi_{R\downarrow}\psi_{R\uparrow} + \text{H.c.}], \tag{8}$$

where we have now suppressed the band index. The scattering rate from Umklapp scattering can be extracted from the imaginary part of the electron's self-energy, $\Gamma(\omega,T) = \text{Im}\Sigma(\omega,T,k_F)$. To lowest order there is a single diagram for each of the three Umklapp interactions, which give identical contributions. One finds

$$\Gamma(\omega,T) = \frac{3}{8\pi}(u_N a_0/v)^2 T\tilde{\Gamma}(\omega/2T), \tag{9}$$

where $\tilde{\Gamma}(X)$ is a scaling function which approaches 1 as $X\to 0$, and varies as $|X|$ for large X. If we ignore vertex corrections, the Kubo formula for the 1D conductivity can be expressed in terms of Γ as

$$\sigma = \frac{8ve^2}{\hbar}\int_{-\infty}^{\infty}\frac{d\omega}{2\pi}\frac{(-\partial_\omega f)}{\Gamma(\omega,T)}, \tag{10}$$

where $f=(e^{\beta\omega}+1)^{-1}$ is the Fermi function. The resulting 1D resistivity is

$$\rho(T) = \frac{c}{16\pi}\frac{h}{e^2}(u_N a_0/\hbar v)^2(T/\hbar v), \tag{11}$$

with c a dimensionless constant of order one.

One of the most promising recent experiments[3] studied single-wall carbon nanotubes packed together into a triangular lattice to form crystalline ''ropes.'' These ropes have diameters of 50 to 200 Å, are tens to hundreds of microns long, and are believed to be predominantly composed of (10,10) armchair tubes. Transport data on a single rope reveals a resistivity increasing linearly with temperature between 50 and 300 K, consistent with metallic behavior. At lower temperatures the resistivity appears to saturate, perhaps turning up slightly but showing no compelling sign of a sizeable charge gap.

A comparison with these results can be made by converting Eq. (11) to the 3D resistivity $\rho_{3d}\approx\rho D^2$, where D is the nanotube diameter. This gives the rough estimate $\rho_{3D}\sim 2(u/t)^2(T/t)\mu\Omega$ cm. Notice that the nanotube size N has dropped out. In the experiments, $d\rho_{\text{exp}}/dT\approx 10^{-2}$ $\mu\Omega$ cm/K. To account for this magnitude one would need a rather large bare Hubbard interaction, $u/t\sim 10$, perhaps not unreasonable given the neglect of long-ranged Coulomb forces in our simple Hubbard treatment. The finite residual resistivity as $T\to 0$ is presumably due to disorder. For example, local kinks or other defects in the rope packing would naturally lead to a temperature-independent additive contribution to the resistivity (see Fig. 5). However, other effects such as 3D crossover may also play a role at low temperatures. Such crossover is influenced by coherent intertube electronic hopping, Coulomb screening from neighboring tubes, and perhaps other effects. More microscopic estimates and/or experimental measures of these couplings are clearly required, and we are pursuing these issues currently.

We are grateful to Chetan Nayak and Doug Scalapino for helpful conversations. This work was supported by the National Science Foundation under Grants No. PHY94-07194, DMR94-00142, and DMR95-28578.

[1] T. W. Ebbesen, Phys. Today **49** (6), 26 (1996).

[2] T. W. Ebbesen *et al.*, Nature (London) **382**, 54 (1996); H. Dai, E. W. Wong, and C. M. Lieber, Science **272**, 523 (1996).

[3] A. Thess *et al.*, Science **273**, 483 (1996); J. E. Fischer *et al.*, Phys. Rev. B **55**, R4921 (1997).

[4] N. Hamada *et al.*, Phys. Rev. Lett. **68**, 1579 (1992); J. W. Mintmire *et al.*, *ibid.* **68**, 631 (1992); R. Saito *et al.*, Appl. Phys. Lett. **60**, 2204 (1992).

[5] X. Blase *et al.*, Phys. Rev. Lett. **72**, 1878 (1994); C. L. Kane and E. J. Mele, *ibid.* **78**, 1932 (1997).

[6] J. Solyom, Adv. Phys. **28**, 201 (1979); A. J. Heeger *et al.*, Rev. Mod. Phys. **60**, 781 (1988).

[7] Y. A. Krotov, D. H. Lee, and S. G. Louie (unpublished).

[8] M. Fabrizio, Phys. Rev. B **48**, 15 838 (1993); R. M. Noack, S. R. White, and D. J. Scalapino, Europhys. Lett. **30**, 163 (1995); L. Balents and M. P. A. Fisher, Phys. Rev. B **53**, 12 133 (1996).

[9] S. A. Kivelson, D. S. Rokhsar, and J. P. Sethna, Phys. Rev. B **35**, 8865 (1987).

[10] See, e.g., E. Dagotto and T. M. Rice, Science **271**, 618 (1996).

[11] R. Noack (private communication).

[12] T. Giamarchi and A. J. Millis, Phys. Rev. B **46**, 9325 (1992).